Laboratory Sands and Natural Siliciclastic Sandstones: Implications for the Behaviour of Reservoirs*

Amanda Murphy[1], Kenichi Soga[2], and Koji Yamamoto[3]

Search and Discovery Article #42165 (2017)**
Posted April 16, 2018

*Adapted from the extended abstract prepared for poster presentation at AAPG/SEG International Conference and Exhibition, London, England, October 15-18, 2017.

[1]Department of Engineering, The University of Cambridge, Cambridge, United Kingdom (aim311@cam.ac.uk) .
[2]Civil and Environmental Engineering, University of California, Berkeley, CA, United States.
[3]Japan Oil, Gas and Metals National Corporation, Tokyo, Japan.

Abstract

A lack of understanding in behavioural differences between sands and sandstones has led to confusion on how to approach and predict the behaviour of sandstone reservoirs, particularly those that are unconsolidated or located at shallow depths. While the geotechnical community has long dealt with the problems of sands, primarily focused on laboratory testing, the petroleum industry has a wealth of geological data from around the world. By plotting this data, the properties of laboratory sands are compared and used as a framework to assess the in situ state and behaviour of natural siliciclastic sandstones.

As granular materials are often one dimensionally compressed in the laboratory (i.e., oedometer test), they show a relationship between the vertical effective stress and porosity (converted to void ratio) and it is called the normal compression line. In laboratory tests at low effective stresses, typically less than 10 MPa for siliciclastic sands, the position of the normal compression line in stress versus void ratio space is dependent upon the initial porosity of the sand. As the vertical effective stress increases these unique curves exhibit a significant change in slope and converge to a single curve called the limiting compression curve (LCC). This slope change is considered to reflect the onset of grain crushing. Compression follows this curve, until at very large stresses the grain packing limit is reached and porosity loss becomes minimal. In contrast to these laboratory results, compaction curves derived from subsiding first-cycle sedimentary basins show a greater porosity loss for the same effective stress compared to the laboratory data. The geological field data and the lab-derived normal compression line diverge at the development of post-sedimentation structures in the form of significant quartz cementation and chemical compaction at around 25 MPa effective vertical stress. The divergence of the field data and the lab-derived normal compression line appears to coincide with a shift in the applicability of critical state failure in soil mechanics to frictional failure (Byerlee's Law).

The position of sandstone reservoirs on the intrinsic compression curve plot has implications for both the study and understanding of these reservoirs and practical field development. Knowing how the reservoir will behave will not only allow for production optimisation of existing fields but could also potentially unlock previously unproducible or uneconomical reservoirs.

Background

Both pressure and temperature increase with depth in sedimentary basins. Typical geothermal gradients range from 10°C/km in stable cratons and 30°C/km in rifting sedimentary basins (Boggs, 2014). Sedimentary basins are generally wide compared to their thickness and the vertical stress is increased as the sediments are buried. This is equivalent to one dimensional compression in the laboratory where the horizontal strains remain zero and vertical stress is increased. Considering that the material behaves as isotropic elastic material, the effective horizontal stress (σ'_H) which develops as a result of this burial is given by:

$$\sigma'_H = \nu/(1-\nu) \text{ x } \sigma'_v \quad (1)$$

where $\sigma'v$ is the vertical effective stress and ν is Poisson's Ratio. This ratio of horizontal to vertical effective stress is often expressed as the coefficient of lateral earth pressure (K_0). In soil mechanics , the compression is plastic deformation dominant and hence use of some material properties related to plastic deformation is more appropriate. Typically, a friction angle is used to estimate K_0 the according empirical equation proposed by Jaky (1944):

$$K_0 = 1-\sin\varphi_{crit} \quad (2)$$

where φ_{crit} is the internal friction angle. In this one dimensional compression the mean effective stress (p') and deviator stress (q) are given by:

$$p' = (\sigma_{v'}+2\sigma_{H'})/3 = (1+2K_0)\sigma'_v/3 \quad (3)$$
$$q = (\sigma_v-\sigma_H) = (1-K_0)\sigma'_v \quad (4)$$

The vertical effective stress (σ'_v) increases with depth and is linked to the density of the sediments. A common approximation for this lithostatic gradient is 1.0 psi/ft (0.023 MPa/m) which reflects a general average density for clastic sedimentary rock of 2.3 g/cm3 (Zoback, 2007). The pore pressure gradient is often approximated by the freshwater gradient of 0.433 psi/ft (0.01 MPa/m). Using these assumptions, typical effective pressures can be calculated for a subsiding first-cycle sedimentary basin.

The Normal Compression Line and Critical State Line

The normal compression line is the relationship between the vertical effective stress ($\sigma\sigma'vv$) and porosity upon first compression of freshly deposited sediments. This relationship is important in geotechnical engineering because it is used to predict the interaction of structures with the ground. An idealised version of the siliclastic normal compression line is shown in Figure 1. The convention in soil mechanics is to report porosity (φ) as a void ratio (e); the volume of voids per unit volume of solids. The conversion between void ratio and porosity is given by:

$$e = \phi/(1-\phi) \quad (5)$$

Granular materials have no unique normal compression line at low effective stresses (less than 10 MPa) and the position depends on initial porosity or void ratio. The observed void ratio reflects the initial conditions of deposition and is limited to a range given by the e_{max} and e_{min}. These are considered to be intrinsic properties of the sand reflecting its particle shape, gradation and angularity and represent the physical limits for grain packing. Void ratios close to the e_{max} represent loosely packed sands and those close to e_{min} represent densely packed sands. The grain packing continues to influence the behaviour of the sand during compression until at high stresses the unique normal compression lines converge to a single normal compression line (Figure 1). This single line is called the limiting compression curve (LCC) (Pestana and Whittle, 1995). The LCC is thought to represent a change from rearrangement of the grains to grain crushing. The stress where this change occurs is often called the yield point or aggregate grain crushing strength (p*). If sediments which have reached the LCC are subsequently unloaded and reloaded, they will follow a non-unique unloading-reloading line. This line is a thin loop which recovers only the elastic deformation before the limiting compression curve. On reloading, this line will be followed until the LCC is reached at the point where the sands experienced the previous greatest stress (p^*_{max}). The compaction will then again follow the LCC (Figure 1). It is interesting that the three diagenetic regimes of Worden and Burley (2009) occur in similar ranges to the different phases of the normal compression line. Eogenesis may be linked to the unique normal compression lines, mesogenesis to the limiting compression curve and telogenesis to the unload-reload cycles.

Critical state in soil mechanics refers to a state where shearing or deformation can continue at constant volume (Schofield and Wroth, 1968). Each sand has a unique critical state line (CSL) which defines the critical void ratio/porosity for a particular pressure that the sand will deform with a constant volume upon shearing (Figure 1). The critical state void ratio at the lowest stresses is often greater than the initial void ratio. In this region all sands dilate. Conventional triaxial compression tests conducted by Lee and Seed (1967) over a pressure range of 0.1 to 10 MPa suggest the critical state line then cuts across the normal compression lines. In this region there is a transition from dilation of the sands to contraction. Looser sands will cross the critical state line first, so in this region loose sands will tend to contract and dense sands dilate when sands are sheared. At high stresses typically greater than 10 MPa, there is a marked increase in slope of the critical state line and the line parallels the normal compression line in a similar way to the critical state line for clays in the Cam Clay model (Been et al., 1991; Muir Wood, 1990; Schofield and Wroth, 1968) (Figure 1). In this region all sands will compact, and if the sand has reached the yield point, this compaction is likely to involve grain crushing.

A number of critical state lines for laboratory sands have been estimated in shearing experiments using a triaxial test apparatus. Mineralogy appears to play a role in the location of the critical state line. Quartzose Leighton Buzzard Sand exhibits a higher void ratio for the same pressure compared to the quartz and feldspar Toyoura, Thanet and Sacramento River sands (Klotz and Coop, 2002; Lee and Seed, 1967). Alvarado et al. (2012) found that the location of critical state line does not seem to be influenced by cementation as the cement bonds are broken during shearing.

The earth's crust has failed throughout geological history and movement typically occurs along pre-existing faults and fractures. This suggests that frictional sliding on a pre-existing fracture may occur before the shear failure of sediments to critical state. Byerlee (1978) collected experimental data on the maximum friction for a variety of igneous, metamorphic and sedimentary rocks and found that the coefficient of friction (μ) was extremely variable at low pressures (< 5 MPa). He attributed this range to differences in rock type and the surface roughness of the contact. At intermediate pressures (5 MPa to 200 MPa) and high pressures (>200 MPa) the friction becomes independent of rock type and surface roughness and can be approximated by Byerlee's law. Interestingly this converging of the friction data occurs at pressures just before

grain crushing in normal compression (Figure 1). Rutter and Glover (2012) converted Byerlee's data to mean effective stress and differential stress plots and found that the critical state slope plots below the friction slope. It is unclear why there is this change to frictional failure. Pre-existing fractures often lack any cohesion (Twiss and Moores, 2007), and it may be that additional cohesion may encourage brittle fracturing.

Experimental Compaction

The geotechnical community has long investigated the properties of sands in the laboratory. Research on the one dimensional compression of sands to high pressures has been carried out by a number of researchers and their findings are summarised below and in Figure 2. Yamamuro et al. (1996) carried out one dimensional compression laboratory tests up to 850 MPa on quartz sand, gypsum sand and Cambria sand (lithic grains) using three different initial porosities for each sand type (Figure 2). The location of the start of the LCC appeared to be related to the mineral hardness of the sands. Quartz required a higher confining stress before the normal compression lines merged to the LCC. The softer gypsum sands only required 2 MPa confining stress before the LCC was reached. The minimum void ratio at a confining stress of 850 MPa was also lower for the softer gypsum sand (Void Ratio: 0.02, Porosity: 2 %) compared to the Cambria (Void Ratio: 0.07, Porosity: 7 %) and quartz sand (Void Ratio: 0.13, Porosity: 12 %). The appearance of the specimens at the conclusion of testing also appeared to be related to the mineralogy. The quartz sand showed extensive crushing and fracturing whereas the gypsum sand appeared to have deformed plastically into the void spaces. Pestana and Whittle (1995) found a similar mineralogical control on the limit for grain crushing from one dimensional compression tests on carbonate, feldspar and quartz sand over a range of pressure from 1 to 100 MPa (Figure 2). Coop and Lee (1993) also reported variation in grain breakage for differences in mineralogy in both one dimensional compression and in isotropic compression. The stress level at which significant breakage occurred in Dogs Bay Sands (biogenic carbonate) was around 0.1 MPa and the Ham River Sand (silica) saw breakage at 1.5 to 2 MPa.

Nakata et al. (2001) examined the influence of sand sorting on the normal compression line up to a confining stress of approximately 100 MPa using one dimensional compression of silica sand (Figure 2). The uniform well sorted samples show a very clearly defined yield point (p_1*) with a much steeper curve after the yield point was reached. Poorly sorted samples have a less well defined yield point. Despite the differences in sorting all the silica samples merge into the LCC above 50 MPa. Altuhafi and Coop (2011) carried out similar research on the effect of particle sorting on the normal compression line using Dog's Bay Sand (biogenic carbonate), Leighton Buzzard Sand (silica) and Langjokull glacial sediment (basaltic sand). The tests subjected the samples to one dimensional compression up to 107 MPa. Altuhafi and Coop (2011) reached the same conclusion for these samples. For more poorly sorted samples the LCC becomes flatter (less steep) and the yield point (p*) is less pronounced. It is thought this difference in slope is due to large amounts of early grain breakage in poorly sorted sands (Altuhafi and Coop, 2011). Beard and Weyl (1973) found that well sorted sands have essentially the same porosity regardless of grain size. For a perfectly sorted sandstone, grain size has no impact on porosity due to the scale independence of grain packing. This similarity appear to extend to the normal compression line as compaction of coarse-grained and fine-grained 50 % quartz and 50 % green shale samples by Pittman and Larese (1991) also showed that different grain sizes with uniform grading had almost identical normal compaction curves. This matches the results of Nakata et al. (2001) which suggest that the initial void ratio (porosity) is important in determining the location of the line and the sorting of the grains causes variation in the shape. The angularity of grains is also likely to play a role in the shape of the normal compression line. More angular grains tend to produce looser packing and higher porosities. Fluid type and grain fabric are also thought to have an influence on the location of the line (Pittman and Larese, 1991).

Compaction Curves from Sedimentary Basins

There is a large volume of literature on the relationship between depth and porosity in sandstone reservoirs (Ehrenberg, 1990, 1995; Houseknecht, 1987; Lundegard, 1992; Magara, 1980; Rittenhouse, 1971). Primary porosity loss during burial diagenesis is attributed to mechanical compaction, chemical compaction and cementation (Houseknecht, 1987). Mechanical compaction is the reorientation, repacking and fracturing of grains. Paxton et al. (2002) suggests that the lower limit to this compaction is 26 % porosity (void ratio of 0.35) and corresponds to the rhombohedral grain packing described by Graton and Fraser (1935). Chemical compaction is the pressure dissolution of framework grains at their points of contact, generally at sharp edges or grain irregularities, and causes both closer packing and reduction in the volume of the grains themselves. Cementation is the precipitation of minerals in the pore spaces available between grains and will reduce the porosity below the mechanical and chemical compaction trends (Houseknecht, 1987).

Petrographical techniques can be used to quantify the relative contribution of mechanical compaction, chemical compaction and cementation to the porosity observed in sandstone reservoirs. Intergranular volume (IGV) is the sum of the pore space, intergranular cement and depositional matrix (clay and silt) and can be used to estimate the mechanical compaction by point counting each of these elements in thin sections. Paxton et al. (2002) collected a database of IGV and depth data for rigid grain uncemented sandstones to estimate mechanical compaction trends. Their results show that porosity reduction by mechanical compaction occurred rapidly from 40 % at the surface to 28 % at depths of 1500 m. As the depth increased, the rate of porosity loss from mechanical compaction slowed and stabilised at 26 % for sandstones (Figure 3). They also demonstrated that cementation in samples from the same formations at the same depths led to significant porosity differences. Lander and Walderhaug (1999) analysed the IGV of moderately well sorted Texas Eocene sandstones buried to depths between 500 to 4500 m and with maximum effective stresses ranging from 10 to 50 MPa. They also found that the majority of porosity loss from mechanical compaction occurred at depths of less than 1500 m. This IGV data is plotted in Figure 3 alongside the normal compression lines of Pestana and Whittle (1995) and Yamamuro et al. (1996) and the critical state line from Klotz and Coop (2002) and Rutter and Glover (2012). The maximum of all the IGV data closely matches the LCC. The lower void ratios/porosities compared to pressure may be due to differences in the intrinsic properties of the sand or unidentified cementation or chemical compaction.

Depositional sandstone porosity was measured by Pryor (1973) in a number of different modern environments and found that porosity in the freshly deposited sands ranged from 17 % to 56 %. Dune sands and beach sands had an average porosity of 49 % and point bar sands averaged 41 %. Ramm and Bjorlykke (1994) estimated porosity depth trends for the Norwegian Shelf reservoir sandstones and concluded that chemical compaction explains much of the porosity loss at depths below 2.5 - 3 km. Geothermal gradient also plays a role in porosity loss. The Middle Jurassic Garn Formation, offshore mid-Norway, is a quartzose sandstone buried in an area with a geothermal gradient of 35^{o}C/km and the Tertiary sands of South Louisiana are also quartzose but are in an area with a lower geothermal gradient of 18^{o}C/km. At depths below 1.5 km the porosity vs depth curve for the Garn Formation becomes steeper and porosity reduces more quickly with depth compared to the South Louisiana Tertiary sands (Ehrenberg and Nadeau, 2005). Taylor et al. (2010) also collected depth vs porosity data for the Gulf of Mexico and Offshore Niger Delta and Sanfilippo et al. (1995) published porosity and depth data for the gas-bearing reservoirs of the Northern Adriatic Basin. Zoback (2007) cited depth and porosity data for the Gulf Coast and field data from the Mahakam Delta showing simple compaction to 3 km. The absolute porosity along with depth from these data sets was converted to void ratio and pressure, then plotted against the one dimensional compression lines (Figure 4). Unlike the IGV data reflecting mechanical compaction, the converted porosity data and normal

compression line curves diverge at the expected onset of significant quartz cementation and chemical compaction. From the plot this occurs around 25 MPa.

Ehrenberg and Nadeau (2005) collected data for average porosity vs depth for 30,122 silciclastic petroleum reservoirs across the world. In contrast to the decreasing porosity with depth trend that is characteristic of areas with simple burial histories, low geothermal gradients and clean quartzose sandstones, these data points plot as a cloud. This wide scatter is likely to be a result of cementation and uplift (unloading). Indeed, the maximum porosity of all the silciclastic reservoir data follows the simple burial history curves. This maximum porosity limit is also shown in Figure 4. In addition Ehrenberg and Nadeau (2005) collected data for the Alberta Basin in Western Canada, where Cretaceous sandstones in the basin have been uplifted; up to 2.8 km during the Tertiary. Ehrenberg and Nadeau (2005) corrected this data back to the pre-uplift depths and the resulting curve showed a similar shape to the simple burial history curves (this curve is also shown in Figure 4).

Strength of Sand and Sandstones

Experimental data on the loading of sandstones is predominantly in the form of hydrostatic tests. In one dimensional compression the horizontal strains remain zero and vertical stress is increased; however, in hydrostatic loading the three principal stresses are increased uniformly with constant pore pressure (throughout loading $\sigma_1 = \sigma_2 = \sigma_3$). This is also referred to as isotropic compression. The one dimensional loading normal compression line for sands lies between the normal compression line for isotropic loading and critical state line. As a result the yield point (p*) for the same sands will occur at higher stress in isotropic compression compared to one dimensional compression (Coop and Willson, 2003). Data for the hydrostatic loading of sandstones samples from Coop and Willson (2003), Cuss et al. (2003), David et al. (1994), Scuderi et al. (2015), Tembe et al. (2008), Wong and Baud (2012) and Zhang et al. (1990) is shown in Figure 5. The sandstone isotropic compression data appear to fit well with the unloading - reloading curve and the LCC. There is a distinctive change of slope which signals the onset of permanent compaction (P_c*max). However, when data for hydrostatically loaded sands is plotted with the sandstone data, often the sandstones show additional strength ($P_c*_{max} > p_c*_{max}$). The St. Peter Sandstone is a weakly cemented quartz sandstone that underwent burial to a maximum depth of 1000 to 3000 m in the Permian before being uplifted (Karner et al., 2003; Pittman et al., 1997; Zhang et al., 1990). Zhang et al. (1990) subjected the St, Peter Sandstone to increasing confining pressures with constant pore pressure up to 600 MPa, using a triaxial apparatus. Karner et al. (2003) carried out hydrostatic and triaxial compaction tests on the 250-350 μm sized fraction of sand created from the St. Peter sandstone. Based on the 250-350 μm sand compression the estimated crushing strength ($p_c*_{max)}$ was around 204 MPa. This is significantly less than the crushing strength of the precursor sandstone which is estimated at 340 MPa (Zhang et al., 1990) (Figure 6).

The sandstone data from isotropic compression can also be compared to the one dimensional compression of the sands by considering their yield envelopes. The location of the crushing pressure or effective pressure at onset of permanent compaction (P_1*_{max}) for one dimensional compression can be estimated using the results of triaxial compression tests and an estimate of the internal friction angle. The friction angle can be used to estimate the relationship between mean effective stress (p′) and deviator stress (q) during one dimensional loading and the yield surface data from triaxial compression can be used to estimate the mean effective stress of $_{P1}*_{max}$. This can be converted to vertical effective stress. Considering that the elastic deformation is very small compared to the plastic deformation, the void ratio will be the same as P_c*_{max} in hydrostatic loading. In this study, a friction angle of 29.5 degrees (a typical value for quartz) was used to estimate a slope of $q/p' = 0.73$ for one dimensional loading for simplicity. This line is shown in Figure 1. A comparison of the yield point (P_1*_{max}) where the sandstones reach the

limiting compression curve on reloading and one dimensional compression curve for sands is shown in Figure 7 (orange dots). In a similar way to overpressure it appears that once significant mechanical compaction has occurred it is irreversible and sandstones with void ratios below 0.35 (porosity 26 %) have a similar yield strength to sands. However, for higher void ratios the sandstones can be stronger than the sands. There is also a clear decoupling of the porosity and vertical effective stress relationship and the grain crushing strength (P^*_{max}) which is not seen in laboratory sand data. This difference is likely to be a result of cementation and chemical compaction in the sandstones.

Discussion

Putting together the observations of the normal compression line, critical state line and the natural sediments compression line, one can construct a model of the different phases during siliciclastic compaction (Figure 7). Depositional setting and provenance control the initial grain packing which is influenced by mineralogy, sorting, particle shape and proportion, and distribution of hard and soft grains. This void ratio occurs between the e_{max} and e_{min} of the sediment. As the effective confining pressure is increased the compaction follows a non-unique line. Depositional environment plays a major role, and the precipitation of early cements will decrease the void ratio. The effect of shearing on the sediment at this stage of compression is determined by density of packing of the sediment; relatively densely packed sediment will dilate to the critical state line, whereas relatively loose sediments will contract. When the effective confining pressure reaches the yield point ($p*$), the normal compression will follow the limiting compression curve. Once this curve is reached, relatively loose sediments need to shear to the critical state by cataclastic flow which involves fracturing of the grains. At void ratios above 0.35 where the mechanical compaction limit has not been reached, the presence of cement may shift the yield-limiting compression curve to the right. Depending upon the geothermal gradient in the sedimentary basin, reduction of the void ratio due to quartz cementation is likely to start around 2 km of burial. Grain fracturing will occur with an increase in confining pressure; however, the fractures in quartz grains are likely to be quickly healed or limited by quartz cement. The cohesion of the sediments will also increase and they may be able to withstand further compaction. This cohesion may encourage brittle faulting rather than dilation of the sediments as the frictional resistance along pre-existing fractures and joints may be less than overcoming the cohesion between the grains. Pressure-solution of grains is also likely to reduce the void ratio. Unloading of sediments that have reached the limiting compression curve will not recover the decrease in void ratio along the limiting compression curve, only the compaction along the non-unique normal compression line. Additionally sediments with cement may not recover the decrease in void ratio along the non-unique normal compression line as the cohesion of the cement may lock the framework in place. This cohesion may mean these sediments ’overshoot’ the limiting compression curve on reloading as they will be stronger than the maximum confining pressure they reached in the first loading cycle.

Implications for Sandstone Reservoirs

The position of a sandstone reservoir on the intrinsic compression curve plot may influence the reservoir properties and behaviour. Challenges, such as sand production and subsidence during production, may be better understood in light of whether reservoirs are truly unconsolidated or whether changes to the stress state are destroying weak cements. Shallow reservoirs may also be more accurately predicted by theories of critical state soil mechanics rather than oilfield geomechanics. Possible characteristics of siliciclastic reservoirs in different areas of Figure 7 are hypothesised below:

1. Siliciclastic reservoirs which have not reached the region of the LCC and retain depositional porosities (~<10 MPa/<1 km) are likely to behave as soils. Grain packing will influence behaviour upon shearing and initial porosity will determine compaction trends. Challenges to production are likely to include unconsolidated sediments, and this region encompasses unconventional gas hydrate reservoirs.
2. Reservoirs with relatively high porosities (>26 %) and significant cementation may be prone to considerable compaction and sand production if depletion causes effective stresses to exceed the yield point (P^*_{max}). Stress changes in these reservoirs may need to be carefully managed.
3. In this region relatively high in-situ pressures and relatively lower porosities suggest these reservoirs have undergone a combination of extensive cementation, interlocking of grains and grain crushing and/or chemical compaction. These reservoirs are unlikely to have problems of sand production and compaction; however, they may be more likely to be prone to brittle failure.
4. Reservoirs located in the bottom-left hand-side of Figure 7 are likely to have undergone significant uplift and are likely to exhibit cementation, chemical compaction and/or grain crushing and interlocking.

Conclusions

The location of the normal compression line of sand is dependent upon a number of factors: initial void ratio (influenced by e_{max} and e_{min}), mineralogy/grain hardness, proportion of soft and hard grains, sorting, particle shape and fluid type present in the void. Just like the intrinsic normal compression line, the natural compaction curve reflects an initial phase involving reorientation and repacking of the grains. Depositional attributes, including composition, porosity and sediment texture, affect early compaction. However, as the pressure and temperature increase with depth, cementation and chemical compaction also decrease the porosity, and the natural compaction curve becomes steeper than the laboratory LCC. Despite these differences, the sandstone yield curve is close to or greater than the LCC for sands. As a result the relationship between the porosity (void ratio) and strength appears to break down. Sandstones are therefore likely to mechanically behave as if they were overconsolidated and have porosities that are lower than predicted by the intrinsic normal compression line for laboratory sands. This divergence of the field data and the lab-derived normal compression line appears to coincide with a shift in the applicability of critical state failure in soil mechanics to frictional failure. However, the underlying cause of this shift is unclear.

Assessing the position of sandstone reservoirs on the intrinsic compression curve plot may allow for the prediction of reservoir behaviour and provide a framework to understand challenges to hydrocarbon production. such as solids production and subsidence.

Acknowledgements

This work is part of a JOGMEC funded study into the Wellbore Stability and Reinforcement of Unconsolidated Formation.

References Cited

Altuhafi, F.N., and M.R. Coop, 2011, Changes to particle characteristics associated with the compression of sands: Géotechnique, v. 61, p. 459-471.

Alvarado, G., M.R. Coop, and S. Willson, 2012, On the role of bond breakage due to unloading in the behaviour of weak sandstones: Géotechnique, v. 62, p. 303-316.

Beard, D.C., and P.K. Weyl, 1973, Influence of texture on pPorosity and permeability of unconsolidated sand: AAPG Bulletin, v. 57, p. 349-369.

Been, K., M.G. Jefferies, and J. Hachey, 1991, The critical state of sands: Géotechnique, v. 41, p. 365-381.

Boggs, S., 2014, Principles of sedimentology and stratigraphy (5th edition): Harlow Pearson Education, ii, 564p.

Byerlee, J., 1978, Friction of rocks: Pure and Applied Geophysics, v. 116, p. 615-626.

Coop, M. R., and I. K.Lee, 1993, The behaviour of granular soils at elevated stresses, *in* G. T. Houlsby, and A.N. Schofield, editors, Predictive Soil mechanics: London, Thomas Telford, p. 186-198.

Coop, M.R., and S.M. Willson, 2003, Behaviour of hydrocarbon reservoir sands and sandstone: Journal of Geotechnical and Geoenvironmental Engineering, v. 129, p. 1010-1019.

Cuss, R.J., E.H. Rutter, and R.F. Holloway, 2003, The application of critical state soil mechanics to the mechanical behaviour of porous sandstones: International Journal of Rock Mechanics and Mining Sciences, v. 40, p. 847-862.

David, C., T.F. Wong, W.L. Zhu, and J.X. Zhang, 1994, Laboratory measurement of compaction-induced permeability change in porous rocks - Implications for the generation and maintenance of pore pressure excess in the crust: Pure and Applied Geophysics, v. 143, p. 425-456.

Ehrenberg, S., 1990, Relationship between diagenesis and reservoir quality in sandstones of the Garn formation, Haltenbanken, mid-Norwegian Continental shelf: AAPG Bulletin, v. 74, p. 1538-1558.

Ehrenberg, S., 1995, Measuring sandstone compaction from modal analysis of thin sections: how to do it and what the results mean: Journal of Sedimentary Research, v. A65, 369-379.

Ehrenberg, S.N., and P.H. Nadeau, 2005, Sandstone vs. carbonate petroleum reservoirs: A global perspective on porosity-depth and porosity-permeability relationships: AAPG Bulletin, v. 89, p. 435-445.

Graton, L.C., and H. Fraser, 1935, Systematic packing of spheres: with particular relation to porosity and permeability: The Journal of Geology, p. 785-909.

Houseknecht, D.W., 1987, Assessing the relative importance of compaction processes and cementation to reduction of porosity in sandstones: AAPG Bulletin, v. 71, p. 633-342.

Jaky, J., 1944, The coefficient of earth pressure at rest: Journal of the Society of Hungarian Architects and Engineers, v. 78, p. 355-358.

Karner, S.L., F.M. Chester, A.K. Kronenberg, and J.S. Chester, 2003, Subcritical compaction and yielding of granular quartz sand: Tectonophysics, v. 377, p. 357-381.

Klotz, E., and M. Coop, 2002, On the Identification of Critical State Lines for Sands: Geotechnical Testing Journal, v. 25.

Lander, R.H., and O. Walderhaug, 1999, Predicting porosity through simulating sandstone compaction and quartz cementation: AAPG Bulletin, v. 83, p. 433-449.

Lee, K.L., and H.B. Seed, 1967, Dynamic strength of anisotropically consolidated sand: Journal of Soil Mechanics & Foundations Division, v. 93, p. 169-190.

Lundegard, P.D., 1992, Sandstone Porosity loss - A big picture view of the importance of compaction: Journal of Sedimentary Petrology, v. 62, p. 250-260.

Magara, K., 1980, Comparison of porosity depth relationships of shale and sandstone: Journal of Petroleum Geology, v. 3, p. 175-185.

Muir Wood, D., 1990, Soil Behaviour and Critical State Soil Mechanics: Cambridge University Press, p. xxiii, 462p.

Nakata, Y., M. Hyodo, A.F.L. Hyde, Y. Kato, and H. Murata, 2001, Microscopic particle crushing of sand subjected to high pressure one-dimensional compression: Soils and Foundations, v. 41, p. 69-82.

Paxton, S.T., J.O. Szabo, J.M. Ajdukiewicz, and R.E. Klimentidis, 2002, Construction of an intergranular volume compaction curve for evaluating and predicting compaction and porosity loss in rigid-grain sandstone reservoirs: AAPG Bulletin, v. 86, p. 2047-2067.

Pestana, J.M., and A.J. Whittle, 1995, Compression model for cohesionless soils: Geotechnique, v. 45, p. 611-631.

Pittman, E.D., and R.E. Larese, 1991, Compaction of lithic sands - Experimental results and applications: AAPG Bulletin, v. 75, p. 1279-1299.

Pittman, J.K., M.B. Goldhaber, and C. Spöetl, 1997, Regional Diagenetic Patterns in the St. Peter Sandstone: Implications for Brine Migration in the Illinois Basin: U.S. Geological Survey Bulletin2094-A, A17p. .

Pryor, W.A., 1973, Permeability-porosity patterns and variations in some Holocene sand bodies: AAPG Bulletin, v. 57, p. 162-189.

Ramm, M., and K. Bjorlykke, 1994, Porosity/depth trends in reservoir sandstones; assessing the quantitative effects of varying pore-pressure, temperature history and mineralogy, Norwegian Shelf data: Clay Minerals, v. 29, p. 475-490.

Rittenhouse, G., 1971, Pore-space reduction by solution and cementation: AAPG Bulletin, v. 55, p. 80-91.

Rutter, E.H., and C.T. Glover, 2012, The deformation of porous sandstones; Are Byerlee friction and the critical state line equivalent?: Journal of Structural Geology, v. 44, p. 129-140.

Sanfilippo, F., G. Ripa, M. Brignoli, and F.J. Santarelli, 1995, Economical management of sand production by a methodology validated on an extensive database of field data, SPE Annual Technical Conference and Exhibition, Dallas, Texas Society of Petroleum Engineers, ESP 30472-MS.

Schofield, A.N., and P. Wroth, 1968, Critical State Soil Mechanics: McGraw-Hill, 310p.

Scuderi, M.M., H. Kitajima, B.M. Carpenter, D.M. Saffer, and C. Marone, 2015, Evolution of permeability across the transition from brittle failure to cataclastic flow in porous siltstone: Geochemistry Geophysics Geosystems, v. 16, p. 2980-2993.

Taylor, T.R., M.R. Giles, L.A. Hathon, T.N. Diggs, N.R. Braunsdorf, G.V. Birbiglia, M.G. Kittridge, C.I. Macaulay, and I. S. Espejo, 2010, Sandstone diagenesis and reservoir quality prediction: Models, myths, and reality: AAPG Bulletin, v. 94, p. 1093-1132.

Tembe, S., P. Baud, and T.-f. Wong, 2008, Stress conditions for the propagation of discrete compaction bands in porous sandstone: Journal of Geophysical Research, v. 113, B09409, doi:10.1029/2007JB005439.

Twiss, R.J., and E. M. Moores, 2007, Structural Geology: W.H. Freeman, p. xvi, 736p.

Wong, T.-f., and P. Baud, 2012, The brittle-ductile transition in porous rock: A review: Journal of Structural Geology, v. 44, p. 25-53.

Worden, R. H., and S. D. Burley, 2009, Sandstone Diagenesis: The Evolution of Sand to Stone, Sandstone Diagenesis, Blackwell Publishing Ltd., p. 1-44.

Yamamuro, J.A., P.A. Bopp, and P.O. Lade, 1996, One-dimensional compression of sands at high pressures: Journal of Geotechnical Engineering, v. 122, p. 147-154.

Zhang, J., T.-F. Wong, and D.M. Davis, 1990, Micromechanics of pressure-induced grain crushing in porous rocks: Journal of Geophysical Research, v. 95, p. 341.

Zoback, M. D., 2007, Reservoir Geomechanics: Cambridge University Press, 452p.

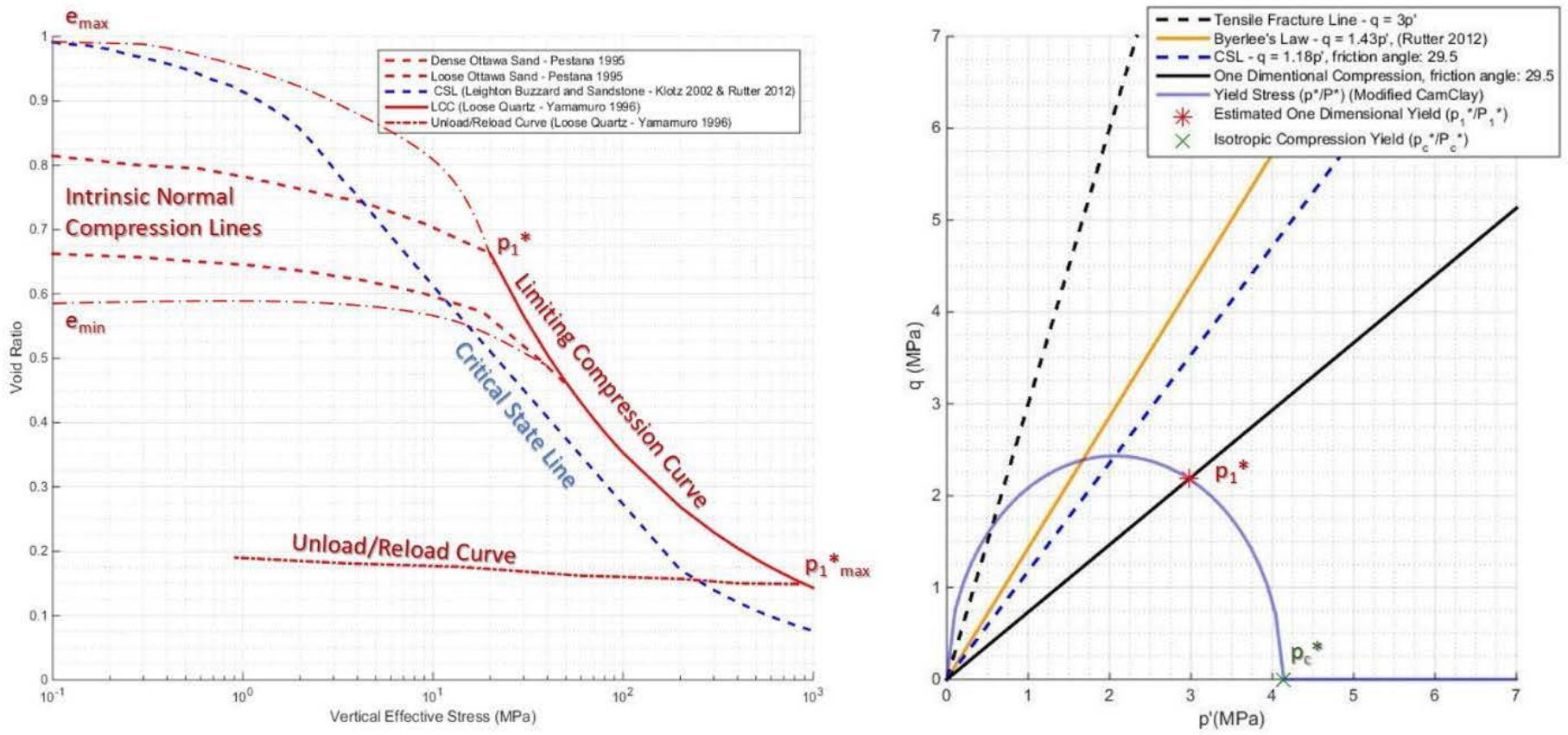

Figure 1. Location of unique normal compression lines, e_{max} and e_{min}, limiting compression curve (LCC), unload/reload curves and critical state line (left). The unload/reload cycle can occur anywhere along the limiting compression curve and will depend upon the location of the sediments on the limiting compression curve when the unloading occurred. Location of the one dimensional compression line, critical state line, Byerlee's law and yield surface in terms of mean effective stress (p ′) and deviator stress (q) (right).

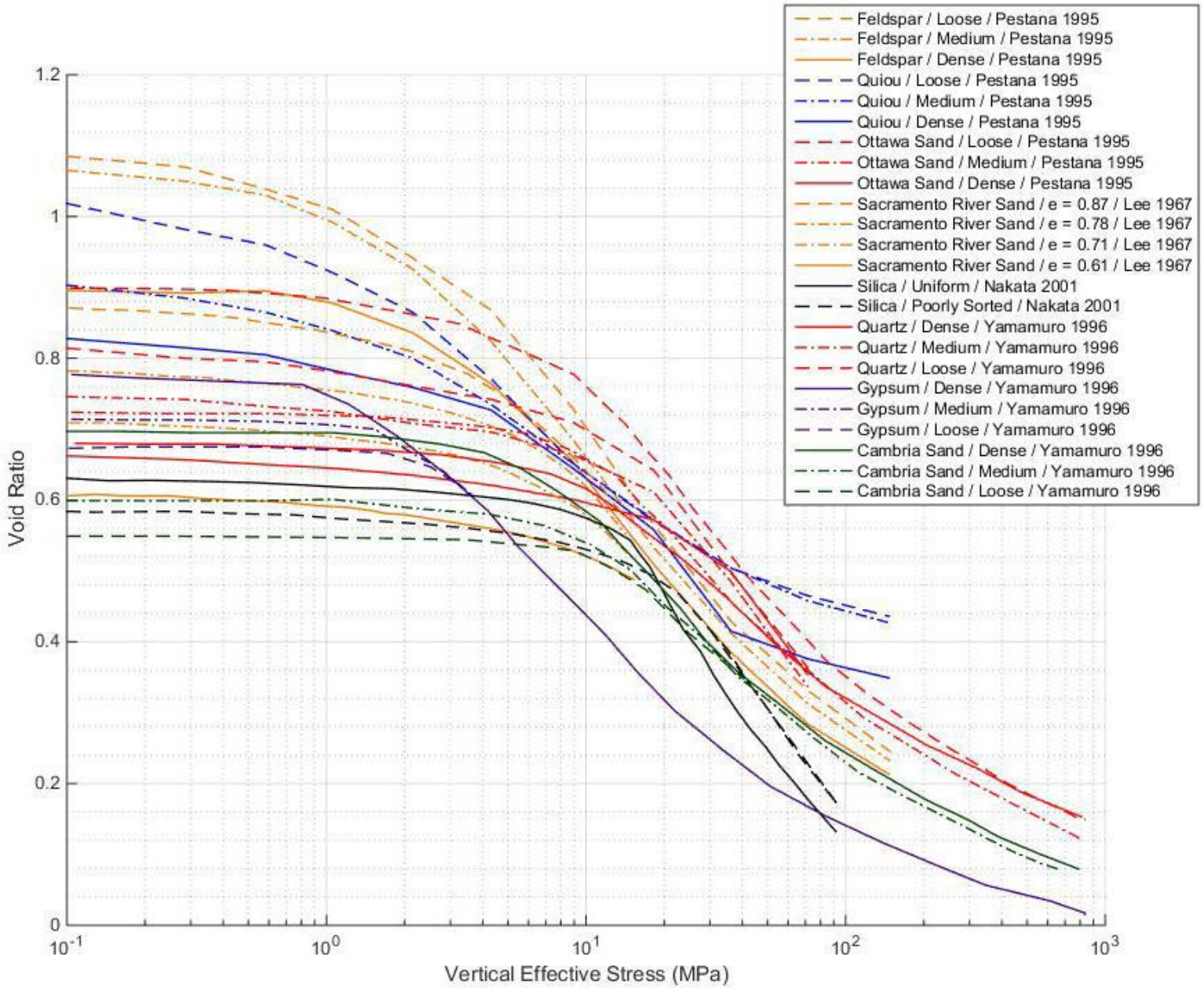

Figure 2. Mineralogy and the Normal Compression Line. Notice later yield point for quartz sands (red and black) compared to feldspar sands (orange) and carbonate sands (blue) and the early yield point for gypsum (purple). Entries in the legend follow the format: "mineralogy/packing/source of the data."

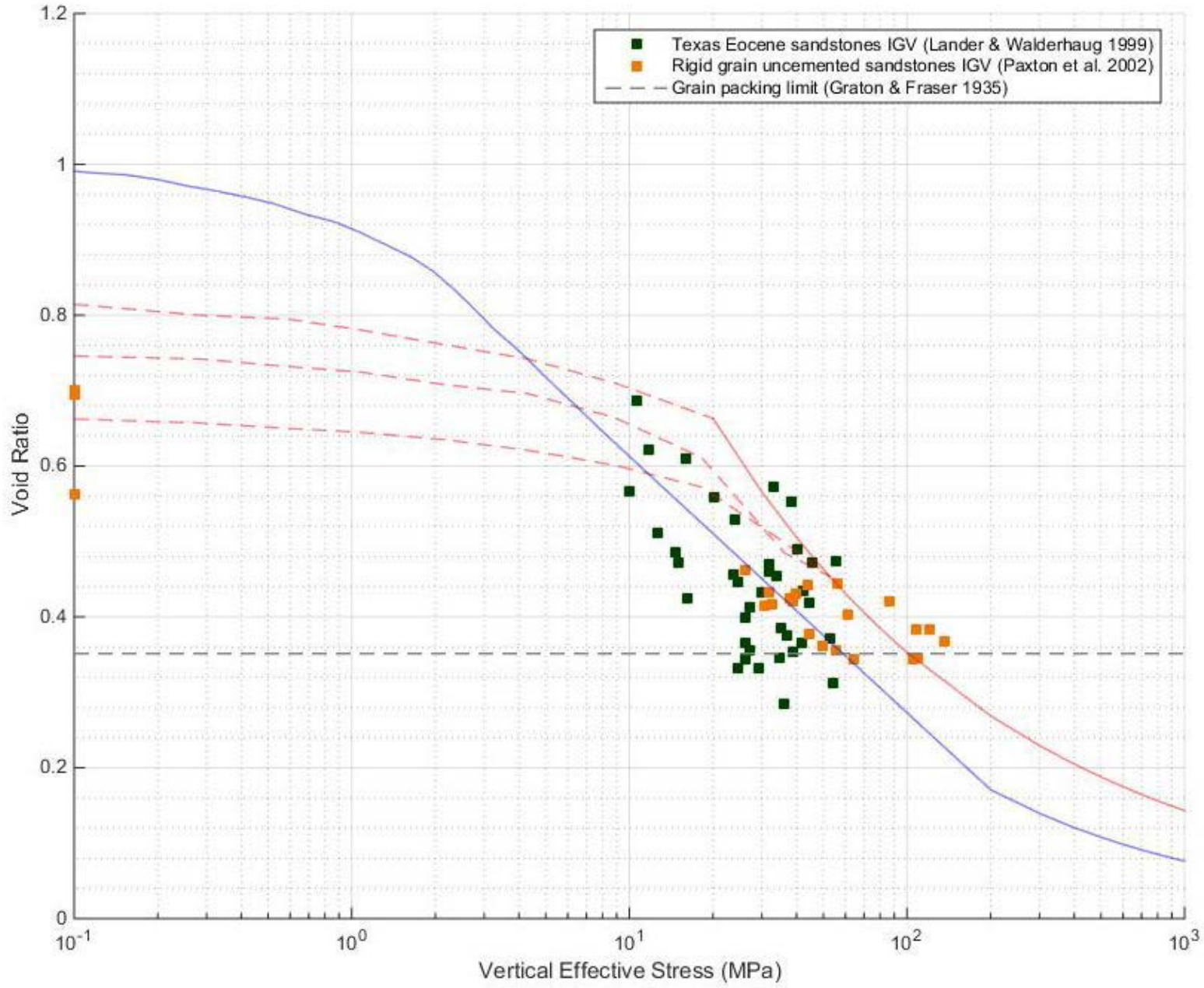

Figure 3. Converted intergranular volume and depth data for sandstones plotted against laboratory one dimensional compression and critical state. Intergranular volume follows the one dimensional compression curve but is limited to the grain packing limit.

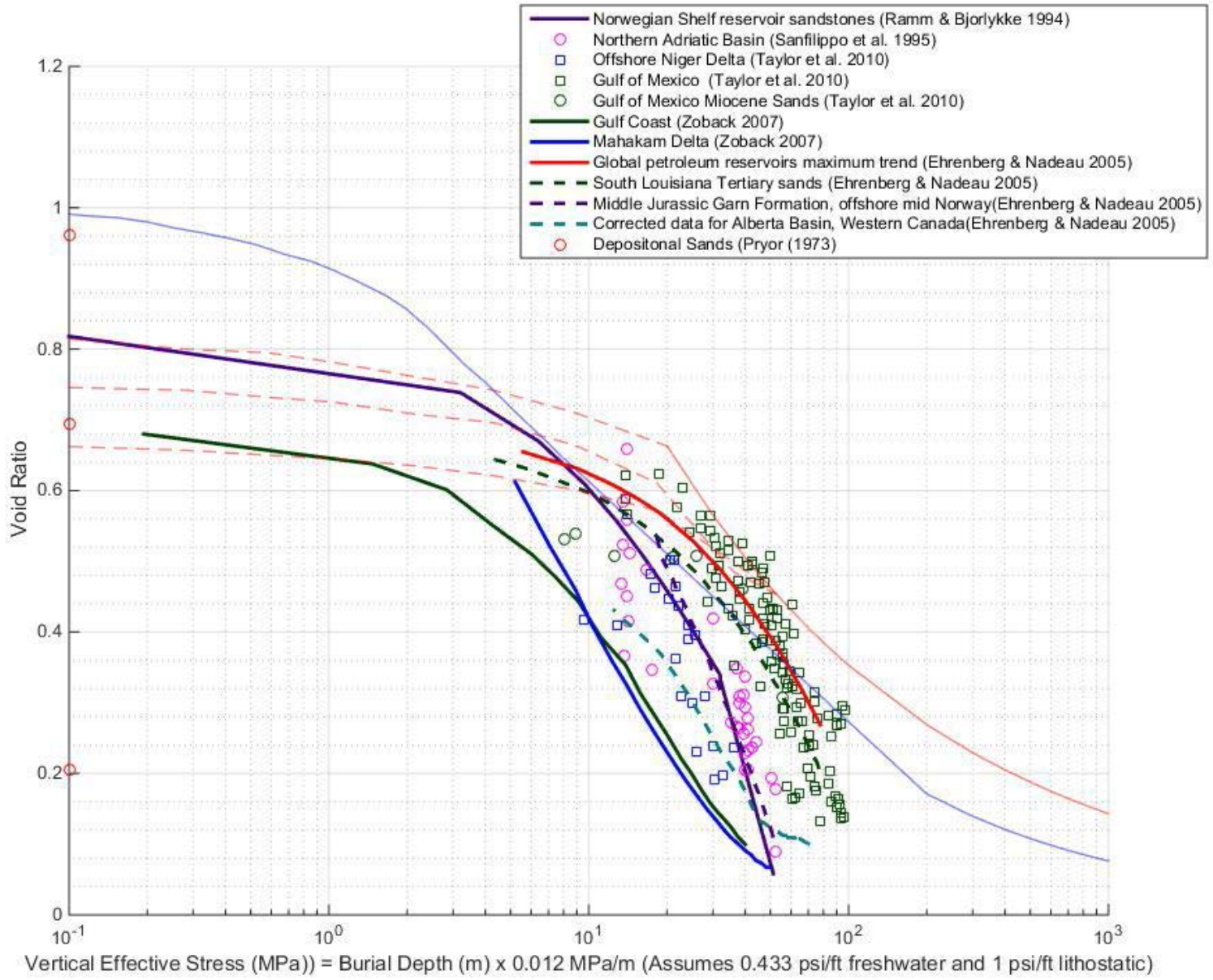

Figure 4. Porosity and depth data converted to void ratio and vertical effective stress. This is plotted with laboratory one dimensional compression data and critical state. The converted porosity data and intrinsic normal compression line diverge at the expected onset of significant cementation and chemical compaction. Geothermal gradient in the sedimentary basin also plays a role in the natural compression curve.

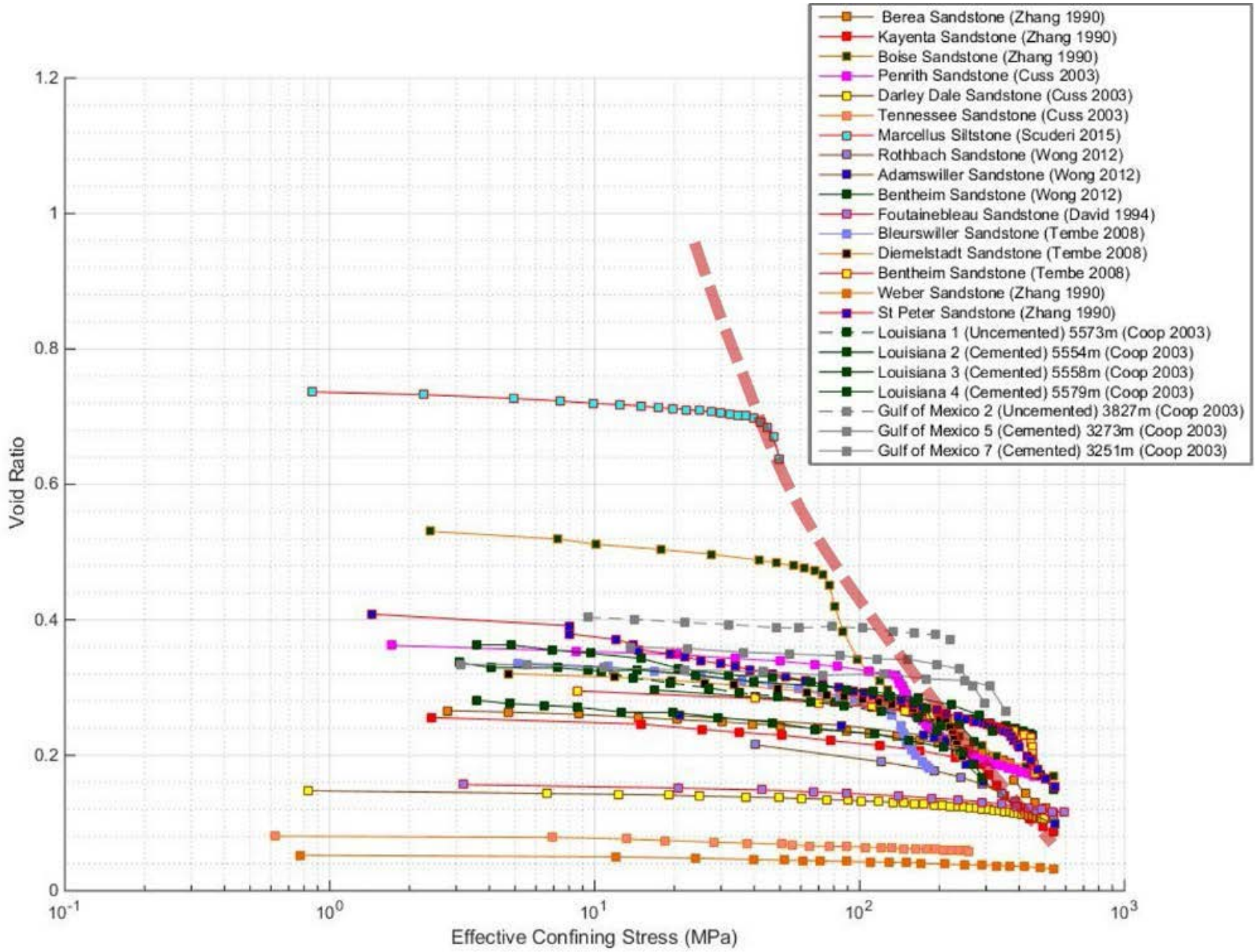

Figure 5. Examples of hydrostatic loading (isotropic compression) of sandstone. The sandstones show a distinctive change in slope of the compaction line which corresponds to the onset of permanent compaction (red dashed line).

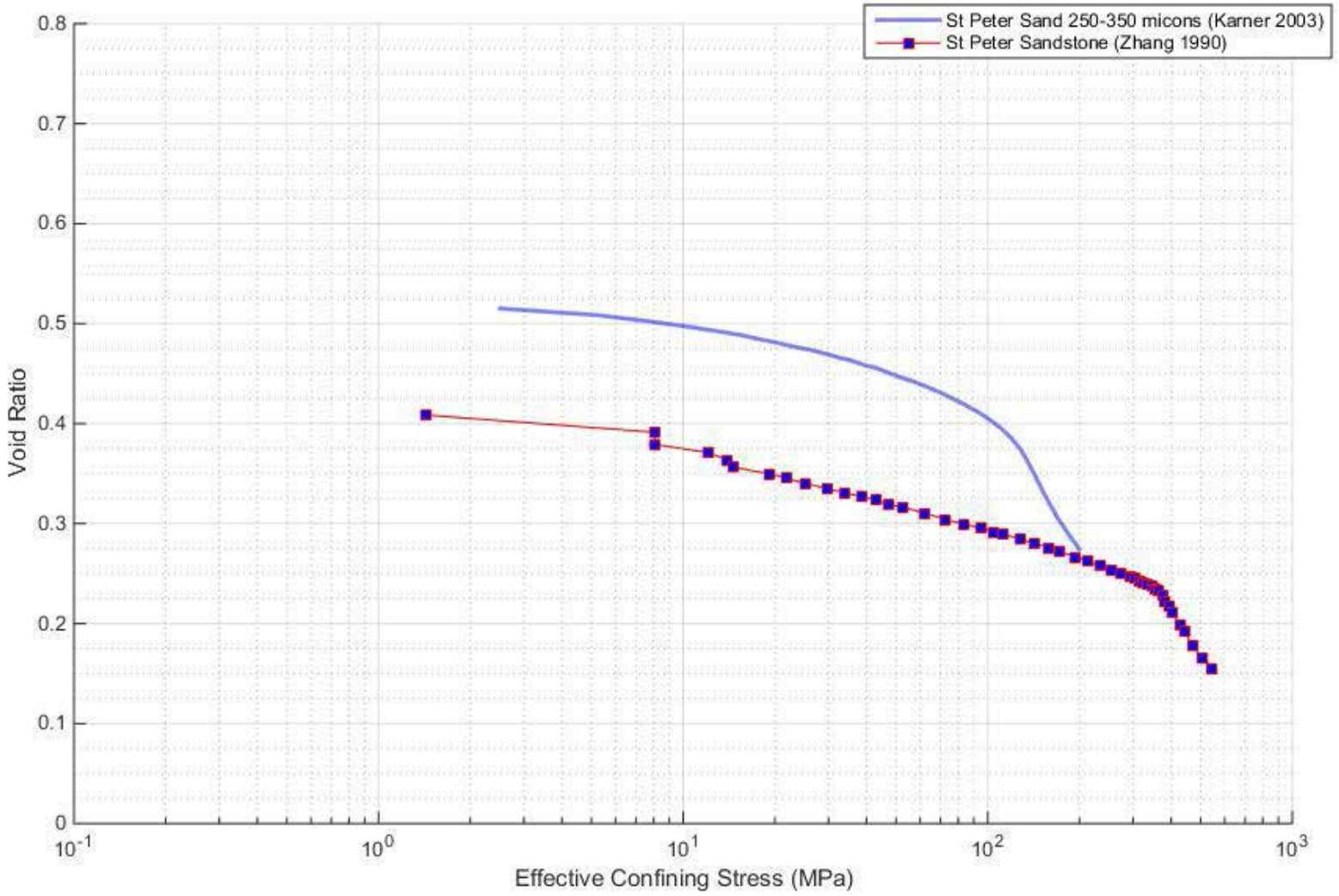

Figure 6. Isotropic compression of the St. Peter Sandstone and 250-350 micron sand created from the sandstone. The St. Peter Sandstone shows a higher crushing pressure than the created sand.

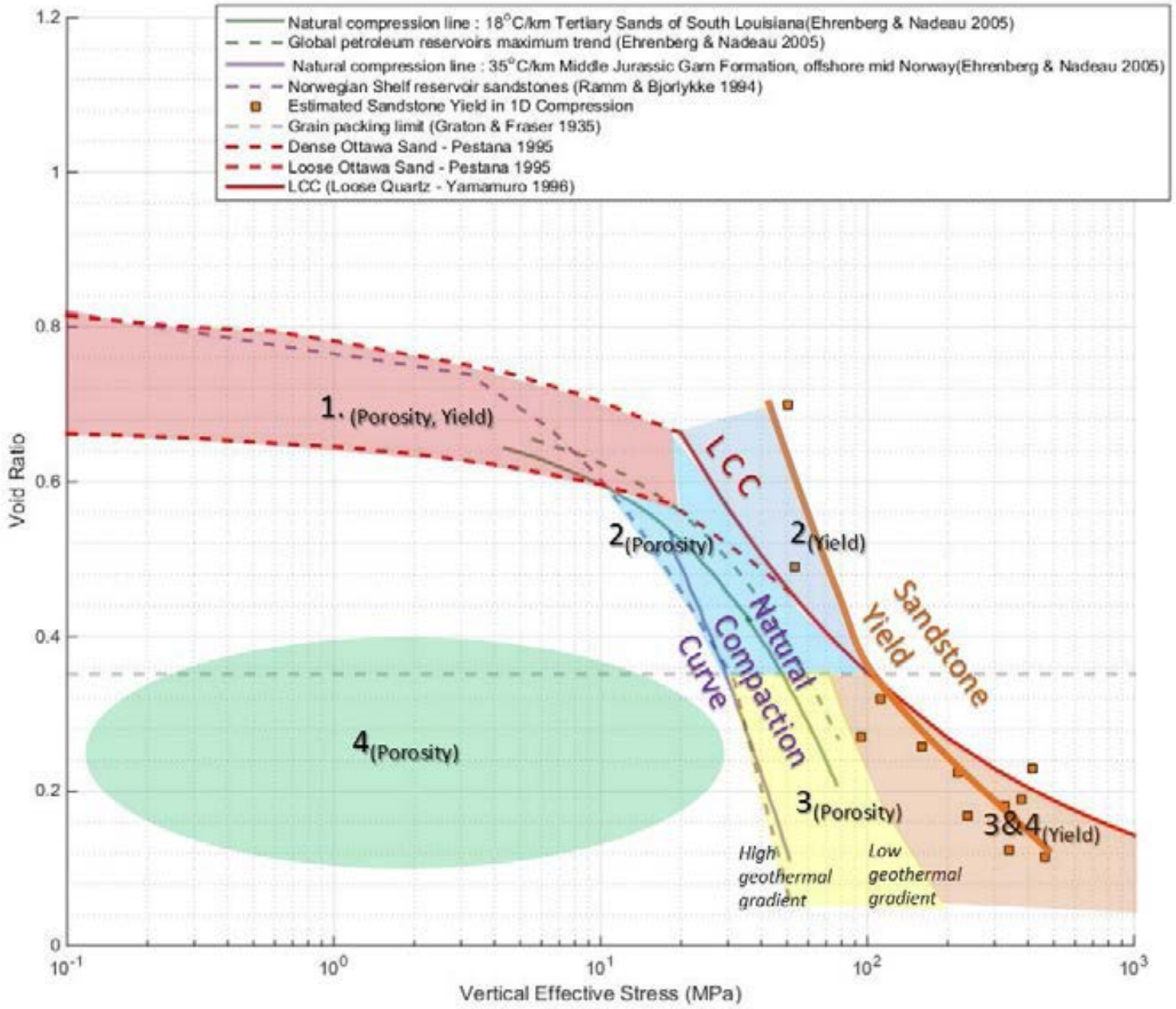

Figure 7. Natural compaction curves, intrinsic normal compression line, and the sandstone yield curve. The natural compaction curve appears to be significantly influenced by the geothermal gradient. The numbers 1 – 4 represent regions on the plot for generalised sandstone reservoir behaviour.